Hybrid position control technique of induction motor drive[*]

by

**Antonio B.S. Júnior, Eber de C. Diniz, Dalton A. Honório,
Luiz H.S.C. Barreto and Laurinda L. N. dos Reis**

Federal University of Ceará
Department of Electrical Engineering
Fortaleza-CE, 60.455-760, Brazil
barbosa@dee.ufc.br

Abstract: This paper presents the study and implementation of a new vector control strategy using a hybrid control technique applied to the mechanical position loop aiming to obtain a system that acts in the fractional horsepower motor driver running at near zero frequency. For this purpose, some control techniques are employed to check which one has the best performance regarding this type of application. The use of three control techniques is considered: the Proportional-Integral-Derivative (PID) controller with fixed gain; the Generalized Predictive Control (GPC) controller; and a hybrid controller. The last one behaves as both PID and GPC using fuzzy logic in order to achieve improved system performance. Simulation and experimental results are shown and discussed to demonstrate the merits of the proposed approach.

Keywords: vector control, predictive control, hybrid control, fuzzy logic

1. Introduction

Induction machines (IM) are widely used in industry due to simplicity, lower cost, reduced need for maintenance, and also greater robustness in comparison with other types of electrical machines. The main difficulty of using the IM for position control is the mathematical modeling of the controller design. Typically, position control of the motor shaft is performed by employing DC motors and servomotors (Bose, 2001).

In the last two decades, advances have occurred in the study of principles that govern vector control applied to alternating current (AC) machines. Therefore, the control of induction machines can achieve performances similar to those of DC motors. The currents and voltages of the IM, using vector control, allow for

the direct control of the spatial orientation of electromagnetic fields, resulting in the use of the term field-oriented for this type of controller. In this type of control, a direct analogy can be established with the control of a DC motor with separate excitation (Bose, 2001).

There are several techniques for speed control applied to IM drives, such as the use of predictive strategies. De Santana, Bim and do Amaral (2008) use the predictive model to control both the speed and rotor flux. Additionally, Beerten, Verveckken and Driesen (2010) use a strategy applied to the predictive scheme in the direct torque control (DTC) to decrease flux and torque ripple. Adaptation techniques are widely used by Jacobina et al. (2003), who apply the strategy named model reference adaptive control (MRAC) to control speed in the IM.

Recently, control strategies that mix various types of controllers have been proposed by several researchers in order to achieve the best performance for each controller, these techniques being known as hybrid control. Ho and Yeh (2010) use a hybrid PID controller, the main characteristics of this controller being the use of a fuzzy controller to tune the PID with the goal of improving the system robustness. Halbaoui, Boukhetala and Boudjema (2008) propose a new robust MRAC using a hybrid strategy. The authors use fuzzy logic to achieve the hybridization between sliding mode control (SMC) and a PI controller for flux and speed control in the IM.

In order to control the position shaft in IMs in a quasi-zero speed operation, a proper strategy is necessary and studies regarding this subject are rarely found in literature. Raute et al. (2010) propose a sensorless control for the IM using harmonic pulse width modulation (HPWM). Ying-Yu (1996) uses the strategy referred to as internal model control (IMC) to achieve zero speed, while Egiguren and Oscar (2010) use variable structure control (VSC) with adaptive gain in the speed loop for the positioning of IM. Won, Kim and Bose (1992) use fuzzy logic to control the IM. Previous works of the present team of authors, also included a comparison between SMC and the use of vector control applied to the speed control for the IM operating at low speeds (Hónorio, 2010).

Therefore, this paper proposes the design of the controller that acts on the position loop in order to achieve the positioning of the IM shaft. Firstly, a conventional PID with fixed gain was used, where fast changes of position reference are considered, although an oscillating behavior around the reference in steady state takes place. Then, a GPC controller is proposed to mitigate this oscillation, and good results are achieved. However, additional time is necessary to reach the reference shaft position in comparison with the PID controller. In order to aggregate the desirable characteristics of both controllers, fuzzy logic was used in combining the PID and GPC controllers for good tracking and low oscillations around reference, respectively.

The technological contribution of this study lies in the possible applications to robotics. So, inexpensive, rugged, and easy to maintain units of induction motors can be used regarding the degrees of freedom of the robot arm, for example. The main scientific contribution consists in the study of a hybrid

control that associates the advantages of two control techniques well known in literature.

Finally, this work presents simulations tests and experimental results in order to demonstrate the main features of the developed system, thus validating the employed methodology. The paper is organized as follows: Section 2 describes the induction motor and its modeling. Sections 3 and 4 present the controller design and the discussion of both simulation and experimental results, respectively. Finally, the proper conclusions are given in Section 5.

2.   Dynamic modeling of the indirect field-oriented control of an induction machine

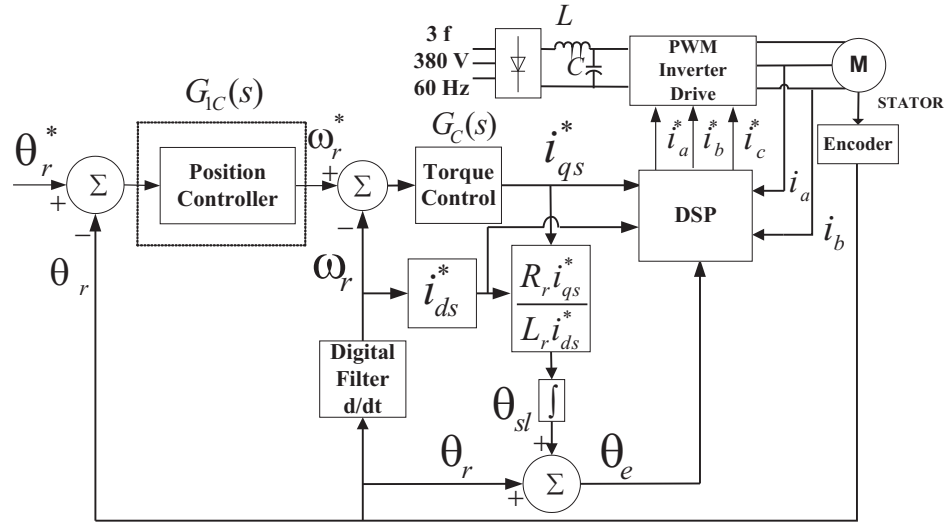The block diagram of the indirect field-oriented induction motor drive is shown in Fig. 1.

Figure 1. Block diagram representing field-oriented induction motor drive

The state space equations of the induction motor in the synchronously rotating reference frame (Bose, 2001) can be described as:

$$\frac{d}{dt}[A] = [B][C] + \frac{1}{\sigma L_s}[D] \tag{1}$$

where:

$$[A] = \begin{bmatrix} i_{ds} \\ i_{qs} \\ \lambda_{dr} \\ \lambda_{qr} \end{bmatrix}; \qquad [C] = \begin{bmatrix} i_{ds} \\ i_{qs} \\ \lambda_{dr} \\ \lambda_{qr} \end{bmatrix}; \qquad [D] = \begin{bmatrix} v_{ds} \\ v_{qs} \\ 0 \\ 0 \end{bmatrix};$$

$$[B] = \begin{bmatrix} -\frac{R_s}{\sigma L_s} - \frac{R_r(1-\sigma)}{\sigma L_r} & \omega_e & \frac{L_m R_r}{\sigma L_s L_r{}^2} & \frac{P\omega_r L_m}{2\sigma L_s L_r{}^2} \\ \omega_e & -\frac{R_s}{\sigma L_s} - \frac{R_r(1-\sigma)}{\sigma L_r} & \frac{-P\omega_r L_m}{2\sigma L_s L_r{}^2} & \frac{L_m R_r}{\sigma L_s L_r{}^2} \\ \frac{L_m R_r}{L_r} & 0 & -\frac{R_r}{L_r} & \omega_e - \frac{P}{2}\omega_r \\ 0 & \frac{L_m R_r}{L_r} & -(\omega_e - \frac{P}{2}\omega_r) & -\frac{R_r}{L_r} \end{bmatrix}.$$

The torque equation is given by:

$$T_e = \frac{3P}{4}\frac{L_m}{L_r}(i_{qs}\lambda_{dr} - i_{ds}\lambda_{qr}) \tag{2}$$

where T_e: electromagnetic torque; R_s: stator resistance per phase; L_s: stator magnetizing inductance per phase; R_r: rotor resistance per phase referred to the stator; L_r: rotor magnetizing inductance per phase referred to the stator; L_m: magnetizing inductance per phase; P: number of poles; ω_e: electrical angular speed; ω_r: rotor angular speed; v_{ds}: d-axis stator voltage; v_{qs}: q-axis stator voltage; i_{ds}: d-axis stator current; i_{qs}: q-axis stator current, and finally, the transient inductance (σ), the q-axis rotor flux linkage (λ_{qr}) and the d-axis rotor flux linkage (λ_{dr}) are given by the expressions (3), (4) and (5), respectively:

$$\sigma = 1 - \frac{L_m{}^2}{L_s L_r} \tag{3}$$

$$\lambda_{qr} = L_m i_{qs} + L_r i_{dr} \tag{4}$$

$$\lambda_{dr} = L_m i_{ds} + L_r i_{qr}. \tag{5}$$

In an ideal field-orientated induction motor, decoupling between d and q-axis can be achieved, while the total rotor flux linkage is forced to align with the d-axis. Accordingly, the flux linkage and its derivative in the q-axis are set to zero as:

$$\lambda_{qr} = 0 \quad \text{and} \quad \frac{d\lambda_{qr}}{dt} = 0. \tag{6}$$

Thus, another rotor flux linkage equation can be found from the third row in (1) and by using (3), namely:

$$\lambda_{dr} = \frac{L_m i_{ds}}{1 + s\frac{L_r}{R_r}}. \tag{7}$$

As the mechanical system is slower in terms of the time constant than the electric system, linearization of the expression (7) can be performed. The time constant $\tau_r = \frac{L_r}{R_r}$ can be considered null. Therefore, expression (7) becomes (8), where the current i_{ds} is considered constant, equal to the desired constant rate rotor flux ($i_{ds} = i_{ds}^*$):

$$\lambda_{dr} = L_m i_{ds}^*. \tag{8}$$

Basing on (3) and (5), expression (2) is simplified to:

$$T_e = \frac{3P}{4} \frac{L_m^2}{L_r} i_{qs}^*$$ (9)

where i_{qs}^* denotes the torque current command generated by the torque controller $G_c(s)$. When using indirect field orientation, the slip angular speed is necessary to calculate the unit vector for coordinate translation. By employing the fourth row of (1) and also (3), the slip angular frequency ω_{sl} can be estimated as:

$$\omega_{sl} = \frac{L_m R_r i_{qs}^*}{L_r \lambda_{dr}} = \frac{R_r i_{qs}^*}{L_r i_{ds}^*}.$$ (10)

The generated torque, rotor speed, and rotor angular position are related by:

$$\omega_r = s\theta_r = \frac{1/J}{s + B/J}[T_e(s) - T_L(s)]$$ (11)

where B is the viscous damping frequency, J is the inertia constant, and T_L is the load torque applied to the shaft.

3. Controller design

3.1. Design of conventional PID controller

There are several methods for tuning PID controllers with fixed gain that are used in the industry with success. Most of these conventional techniques are based on the Ziegler-Nichols method. This paper uses the modified Ziegler-Nichols method technique by reallocating the Nyquist point of the curve (Åström and Hägglund, 1995). The point to be moved is usually the last point of resonance, which can be determined by the relay method. This technique has already been employed in previous works of the present authors (Hónorio et al., 2010).

3.2. Design of generalized predictive controller

The implementation of the predictive controller requires a model for the system under study in order to compute the prediction horizons of control to be used. Therefore, it requires a preliminary study to choose a model that would result in the best matching of the system. Thus, this section describes the modeling for the system and the predictive controller.

3.2.1. System identification

The transfer function of a given system can be identified by using several methods. In this case, the system operates in closed loop (Fig. 2), and some approaches available in literature such as the relay and Ziegler-Nichols methods

(Coelho and Coelho, 2004) and Yuwana and Seborgs method (Aguirre, 2004) have proven to be adequate.

A large majority of industrial process units of the type to be controlled can be adequately approximated by the first-order plus time delay (FOPTD) model (Aguirre, 2004) whose general form is given by (12), where K is the gain of the process model, τ is the time constant of FOPTD process model, and τ_d is the time delay.
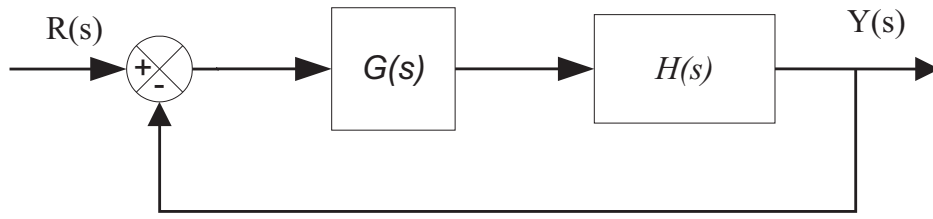
Figure 2. Configuration of the closed loop system

The input of the system is a signal reference of position, which corresponds to a given sector in modulation SVPWM (Space Vector Pulse Width Modulation) used in AC driver, and the output is the actual motor shaft position. Due to the fact that the system does not have any delay in transmission, parameter τ_d is considered null, and one must calculate the proper values for K and τ,

$$H(s) = \frac{Ke^{-\tau_d s}}{1 + \tau s}. \tag{12}$$

Considering that the aforementioned parameters for $H\,s$ are properly determined, expressions (13) to (18) result:

$$K = \frac{y_\infty}{K_c (A - y_\infty)} \tag{13}$$

$$y_\infty \approx \frac{y_{p2} y_{p1} - y_m^2}{y_{p2} + y_{p1} - 2y_m} \tag{14}$$

$$K_f = K_c K \tag{15}$$

$$\tau = \frac{\Delta t}{\pi} \left[\zeta \sqrt{K_f + 1} + \sqrt{\zeta^2 (K_f + 1) + K_f} \right] \sqrt{(1 - \zeta^2)(K_f + 1)} \tag{16}$$

$$\zeta_1 = \frac{-\ln \left[\frac{y_\infty - y_m}{y_{p1} - y_\infty} \right]}{\sqrt{\pi^2 + \left(\ln \left[\frac{y_\infty - y_m}{y_{p1} - y_\infty} \right] \right)^2}} \tag{17}$$

$$\zeta_2 = \frac{-\ln \left[\frac{y_{p2} - y_\infty}{y_{p1} - y_\infty} \right]}{\sqrt{4\pi^2 + \left(\ln \left[\frac{y_{p2} - y_\infty}{y_{p1} - y_\infty} \right] \right)^2}}. \tag{18}$$

Variable ζ, appearing in (16) is the mean value of ζ_1 and ζ_2 from, respectively, equations (17) and (18). The remaining parameters are found by using Fig. 3, i.e. $y_{p1} = 1.7$; $y_{p2} = 1.4$; $K_c = 10$; $y_m = 0.4$; $A = 1$; $\Delta t = 0.7$; $y_\infty = 0.9652$; $K = 2.775$; $K_f = 27.75$; $q_{si} = 0.081$; $\tau = 6.8116$.
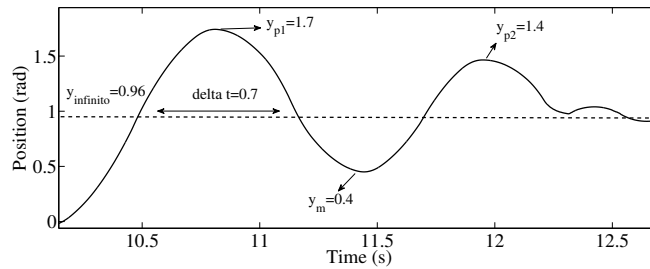

Figure 3. Step response using Yawana and Seborg's method

By using (12), the transfer function in continuous time can be obtained as:

$$H(s) = \frac{2.775}{6.812s + 1}. \tag{19}$$

Assuming zero-order hold (ZOH) and the sampling rate of 0.4 ms, the discrete representation of (19) is:

$$H(z) = \frac{0.000163}{z - 0.9999}. \tag{20}$$

3.2.2. GPC-based I+P controller design

System description

The system description was first considered in (20). The respective discrete-time model is given by

$$A(z^{-1})y(k) = z^{-km}B(z^{-1})u(k-1) + \frac{C(z^{-1})}{\Delta}\xi(k) \tag{21}$$

where $A(z^{-1})$ and $B(z^{-1})$ are polynomials given by:

$$\begin{aligned} A(z^{-1}) &= 1 + a_1 z^{-1} + ... + a_{na} z^{-na} \\ B(z^{-1}) &= b_0 + b_1 z^{-1} + ... + b_{nb} z^{-na} \end{aligned} \tag{22}$$

and $u(t)$, $y(t)$ and $\zeta(t)$ are the control input, the corresponding output signal, and white Gaussian noise with zero mean and variance σ^2. Furthermore, z^{-1} denotes the backward shift operator, which is defined by $z^{-1}y(t) = y(t-1)$, and Δ denotes the differencing operator defined by $\Delta = 1 - z^{-1}$. Equation (21) is the so–called CARIMA (Controlled Auto-Regressive and Integrated Moving Average) model (Clarke, 1987), and is utilized as the controller design oriented

model in this paper.

Controller I+P

As mentioned above, I+P control schemes have been widely used in industrial processes. All the controllers will have the RST structure (Aström and Hägglund, 2006), shown in Fig. 4, where $\Delta = 1 - z^{-1}$, $y_r(t)$ is reference, $u(t)$ control input, and $y(t)$ output of process, $d_{in}(t)$ and $d_{out}(t)$ are corresponding perturbations of input and output, respectively, and $\eta(t)$ is noise.
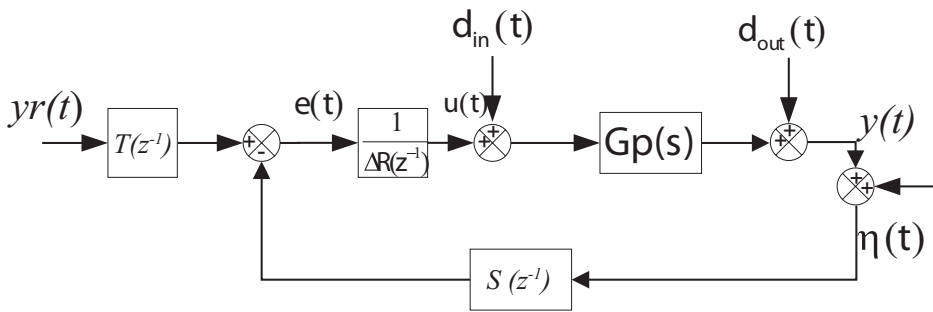

Figure 4. Structure of the RST controller

The controller structure is given by:

$$R(z^{-1})\Delta u(t) = T(z^{-1})yr(t) - S(z^{-1})y(t) \tag{23}$$

where $R(z^{-1})$, $S(z^{-1})$ and $T(z^{-1})$ are polynomials in the backward shift operator z^{-1}. The controller I+P is shown in Fig. 5.
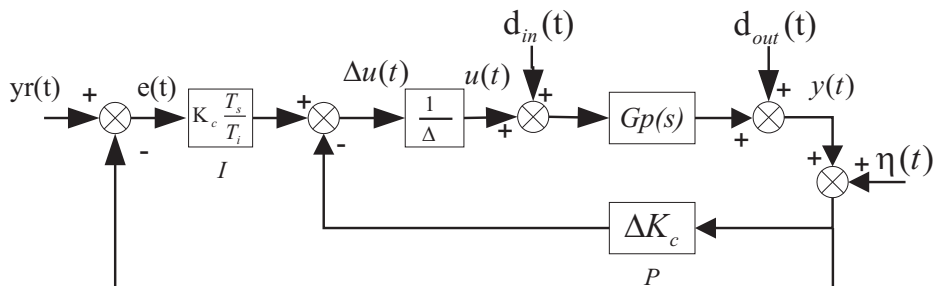

Figure 5. Structure of the I+P controller

The polynomials $R(z^{-1})$ and $S(z^{-1})$ are given by

$$\begin{aligned} R(z^{-1}) &= 1 \\ S(z^{-1}) &= s_0 + s_1 z^{-1} \\ T(z^{-1}) &= S(z^{-1}) \end{aligned} \tag{24}$$

where s_0 and s_1 are:

$$\begin{cases} s_0 = Kc(1+\frac{Ts}{Ti}); \\ s_1 = -Kc. \end{cases} \tag{25}$$

In the RST structure, $R(z^{-1})$ is 1. The polynomials $S(z^{-1})$ and $T(z^{-1})$ are:

$$\begin{cases} S(z^{-1}) = s_0 + s_1 z^{-1} \\ T(z^{-1}) = t_0 + t_1 z^{-1} \end{cases} \tag{26}$$

where s_0, s_1, t_0, t_1 are, respectively:

$$\begin{cases} s_0 = Kc(1 + \frac{Ts}{Ti}) \\ s_1 = -Kc \\ t_0 = Kc(1 + \frac{Ts}{Ti}) \\ t_1 = -Kc. \end{cases} \tag{27}$$

GPC-based PID parameter tuning

One of the GPC unrestricted criteria, which has been proposed by Clarke (1987) is given by

$$J = E\left[\sum_{i=N_1}^{N_y} [y(k+1) - w(k)]^2 + \lambda \sum_{i=1}^{N_u} [\Delta u(k+i-1)]^2 \right] \tag{28}$$

where λ denotes the control weighting factor, and $w(t)$ the reference signal given by piecewise constants. Furthermore, the period from N_1 through N_y denotes the prediction horizon, and N_u denotes the control horizon. For simplicity, they are respectively set as $N_1=1$, $N_y=N$ and $N_u=N$, where N is designed in consideration of the time constant of the controlled object. Minimizing (28) yields the following control law:

$$\sum_{i=1}^{N} k_i F_j(z^{-1})y(t) + \left\{ 1 + z^{-1} \sum_{i=1}^{N} k_i G_i^{\cdot}(z^{-1}) \right\} \Delta u(k) - \sum_{i=1}^{N} k_i yr(t) = 0 \tag{29}$$

where $F_j(z^{-1})$ and $G_i^{\cdot}(z^{-1})$ are obtained by solving the following Diophantine equations:

$$1 = E_i(z^{-1})\Delta A(z^{-1}) + z^{-i} F_i(z^{-1}) \tag{30}$$

and

$$E_j(z^{-1})B_j(z^{-1}) = R_j(z^{-1}) + z^{-1} S_j(z^{-1}) \tag{31}$$

where

$$\begin{cases} E_i(z^{-1}) = 1 + e_1 z^{-1} + ... + e_{i-1} z^{-(i-1)} \\ F_i(z^{-1}) = f_{i,0} + f_{i,1} z^{-1} + ... + f_{i,na} z^{-na} \end{cases} \tag{32}$$

and the polynomials $R(z^{-1})$, $S(z^{-1})$ and $T(z^{-1})$ of the GPC controller in RST are:

$$\begin{cases} R(z^{-1}) = \left[1 + z^{-1} \sum\limits_{i=1}^{N} G_i(z^{-1})\right] \\ S(z^{-1}) = \sum\limits_{i=1}^{N} k_i F_i(z^{-1}) \\ T(z^{-1}) = \sum\limits_{i=1}^{N} k_i \end{cases} \tag{33}$$

where $R(z^{-1})$ is approximated by the static gain, ν, defined as:

$$\nu = 1 + \sum_{i=N_1}^{Ny} k_i G_i(1). \tag{34}$$

Then, equation (29) can be rewritten as:

$$\Delta u(k) = \frac{1}{\nu} \sum_{i=N_1}^{Ny} k_i yr(k) - \frac{1}{\nu} \sum_{i=N_1}^{Ny} k_i F_i(z^{-1})y(k). \tag{35}$$

Hence, the simplified polynomials $\overline{R}(z^{-1})$, $\overline{S}(z^{-1})$ and $\overline{T}(z^{-1})$ of the GPC controller in RST are given by:

$$\begin{aligned} \overline{R}(z^{-1}) &= 1 \\ \overline{S}(z^{-1}) &= \overline{s}_0 + \overline{s}_1 z^{-1} \\ \overline{T}(z^{-1}) &= \overline{t}_0, \end{aligned} \tag{36}$$

where the coefficients $\overline{s}_0$, $\overline{s}_1$, and $\overline{t}_0$ are:

$$\overline{s}_0 = \frac{1}{\nu} \sum_{i=N_1}^{Ny} k_i f_{i,0}, \ \overline{s}_1 = \frac{1}{\nu} \sum_{i=N_1}^{Ny} k_i f_{i,1} \ and \ \overline{t}_0 = \frac{1}{\nu} \sum_{j=N_1}^{Ny} k_j. \tag{37}$$

Then, using equations (25) and (29), the parameters of I+P are given by:

$$K_c = -\overline{s}_1 \ and \ Ti = \frac{-\overline{s}_1}{\overline{s}_0 + \overline{s}_1} Ts. \tag{38}$$

3.3.   Structure of hybrid control using fuzzy logic

The structure proposed in Fig. 6 is used to achieve the mix of the two control techniques. The fuzzy logic is used as weight, i.e. the fuzzy logic increases or decreases the action of each controller in order to obtain the best behavior of the system.

As it can be seen, the output of the fuzzy logic block goes directly to a multiplier block together with the PID. On the other hand, the block, which
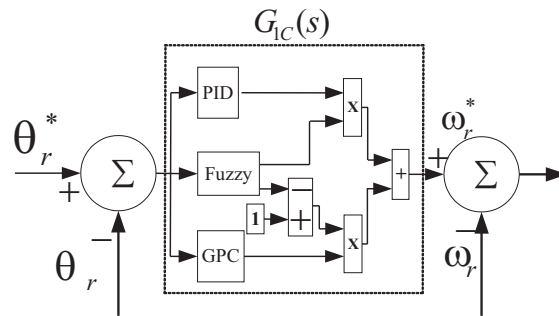
Figure 6. Representation of the proposed indirect field-oriented drive

multiplies the GPC action has complementary fuzzy output because fuzzy logic by definition employs values ranging from zero to unity.

The use of the aforementioned control techniques, i.e. PID and GPC, is justified by simplicity and ease of implementation in an embedded system. For instance, a DSP is used in the proposed approach.

In order to obtain the strategy mixing PID and GPC with the use of fuzzy logic, three different subregions are defined within the control region, these subregions being called SMALL, PID-GPC, and LARGE, as shown in Fig.7, where e is the normalized position error and μ is the degree of membership and each subregion corresponds to a system operational mode.
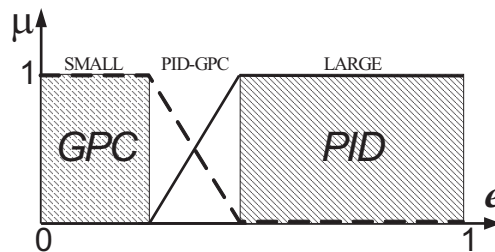

Figure 7. Membership functions used in fuzzy logic

The first strategy corresponds to pure GPC region and it aims to maintain the constant error at a minimum value or to eliminate it. The middle region mixes PID and GPC strategies to produce a unique control signal, the objective of this region being to smooth the eventual overshoot during the reference change. The third and final area involves more of PID than of GPC action, and is responsible for bringing the system to the reference as fast as possible.

4.   Simulation and experimental results

In order to calculate the PID parameters, the modified Ziegler-Nichols technique is used, and the following results are obtained: $K_c = 0.4787$, $T_i = 0.03923$ ms, $T_d = 0.0098075$ ms (Júnior, 2010).

To implement the GPC controller, the parameters $N_y = 10$, $N_u = 10$, $\lambda = 0.1$ and $\nu = 1$ were used, together with the methodology shown in Section 3.2. Resulting from this were the parameters $K_c = 2.6587$, $T_i = 12.79e^{-5}$, $t_0 = -15.1181$, $s_1 = 0.7198$ and $s_0 = -0.2802$.

The fuzzy logic was adjusted empirically in order to appropriately combine the good characteristics of PID controllers, which act instantly when reference is changed, with those of GPC controllers, which behave better after the steady state has been reached.

This study has used MATLAB for the proper configuration of fuzzy logic control. The inference algorithm of Mamdani and the defuzzification method were chosen for the central subregion of Fig. 7, where the fuzzy set represents both the PID and GPC controllers. The fuzzy input is the normalized difference between the reference position and the actual position of the rotor.
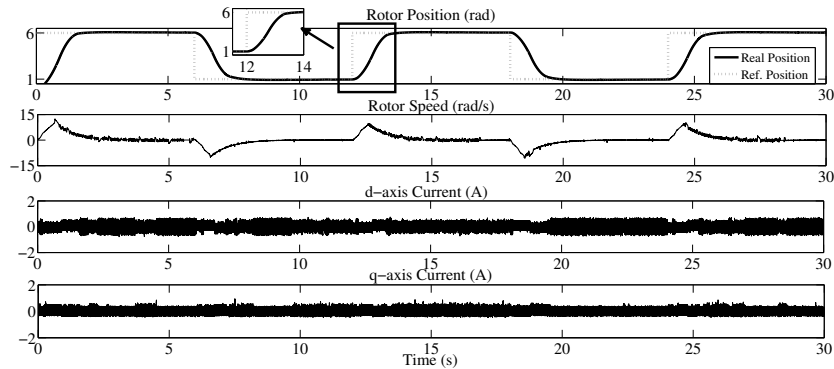

Figure 8. Simulation results for the system using the PID control strategy

The behavior of the rotor position reference is analyzed. The simulation is composed of two steps in the rotor position reference, in the first step the initial value of 6 radians is changed to 1 radian. In the second step the rotor position must change from 1 to 6 radians. It is possible to verify the system capability in terms of accuracy and repeatability of the rotor positioning by changing position each 6 seconds.

Fig. 8 shows the evaluation of the PID control strategy. By observing the tracking position within the time window of 2 seconds, as can be seen in detail for the interval between 12 and 14 seconds, we conclude about the speed of the reference shift. Analyzing the behavior of the rotor speed one can see that there is a small oscillation after reaching the reference. The currents i_d and i_q oscillate with peaks of 0.5 A.

The GPC strategy, used to produce results shown in Fig. 9 takes about 3 seconds to stabilize the reference at 6 radians, see the details appearing during the time interval between 12 and 15 seconds. Concerning the rotor speed there is an almost null oscillation at the reference. The currents show a peak of 1 A.
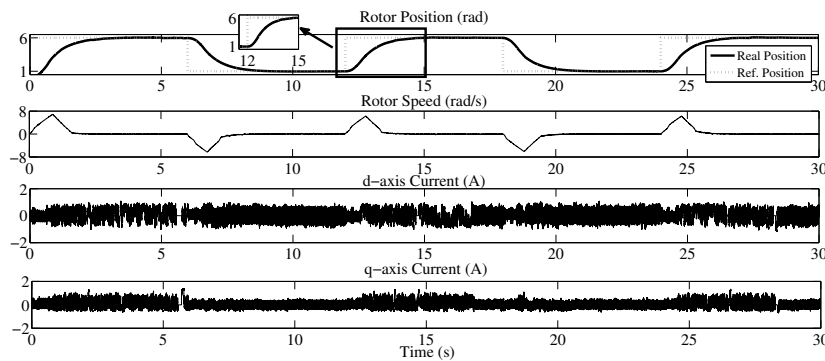
Figure 9. Simulation results for the system using the GPC control strategy

By using fuzzy logic, as it is shown in Fig. 10, one can observe that the response time is slightly longer than for the PID strategy, namely about 2.5 seconds to reach the reference. And it can also be seen that there are small oscillations at the reference, like in the GPC strategy. The variation of the i_d and i_q currents has a peak of 0.5 A.
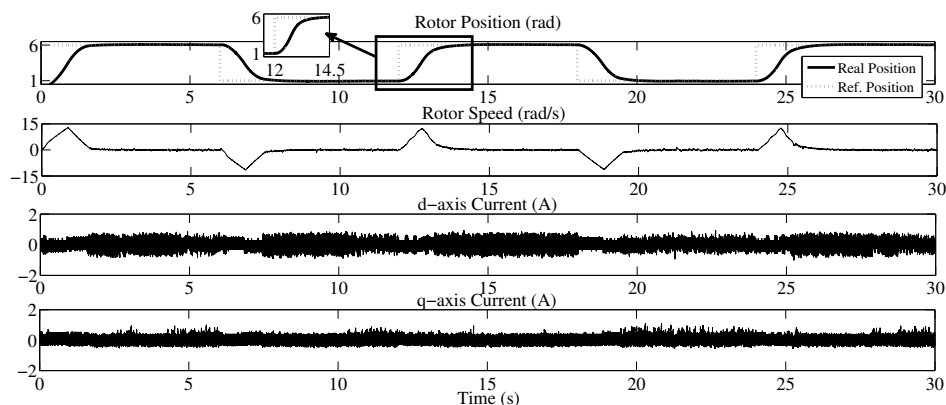
Figure 10. Simulation results for the system using the fuzzy control strategy

For the experimental implementation of the system, a kit consisting of a DSP from *Texas Instruments*, TMS320F2812, was used. The machine is a fractional horsepower three-phase squirrel cage IM, whose parameters are given in Table 1.

Table 1. **Motor parameters**

Parameters	Value
Rated power	0.25 HP
Rated speed	1725 rpm
Rated voltage	220 V
Rated current	1.26 A
Number of poles	4
Rotor resistance referred to the stator	87.44 Ω
Stator resistance	35.58 Ω
Rotor inductance referred to the stator	0.16 H
Stator inductance	0.16 H
Mutual inductance	0.884 H
Inertia moment	$5 \cdot 10^{-4}\ kg \cdot m^2$
Viscous friction coefficient	$5.65 \cdot 10^{-3}\ kg \cdot m^2/s$

The remaining instruments are Hall-effect current sensors, the auxiliary voltage sources, a three-phase voltage inverter module by Semikron with a switching frequency of 2.5 kHz, a multi-turn precision potentiometer coupled to the motor shaft, with a sampling time of 0.4 ms. The experimental setup is shown in Fig. 11.
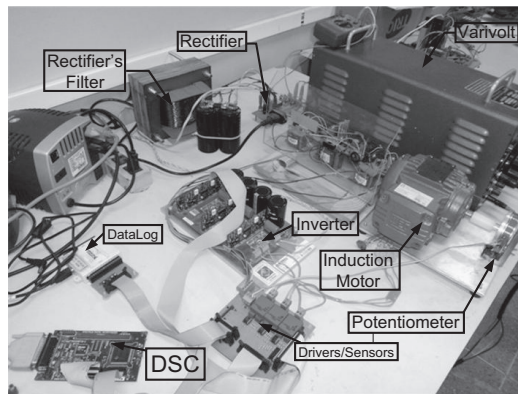

Figure 11. Experimental setup

The same control techniques as those considered in the simulation tests are studied, while the same conditions for the reference step are maintained, i.e. shifts from 6 to 1 radian and from 1 to 6 radians with changes taking place each 6 seconds. Similar performance is verified, with the sole difference concerning the behavior of d_q currents, because the simulation does not take into account the real problems of an experiment, as well as the variation of inertia moment of the system due to the load added to the motor shaft, among other real problems.

Analyzing the results for PID, given in Fig. 12, one can observe that it is the fastest one among the used techniques, taking about 1.2 seconds, view detail A, to reach the reference with some oscillation in the reference around 0.8 radians, detail B. And the rotor speed is quite high, as expected. The current i_{ds} presents the peak of 2 A, while the peak values for i_{qs} are limited to 1 A.
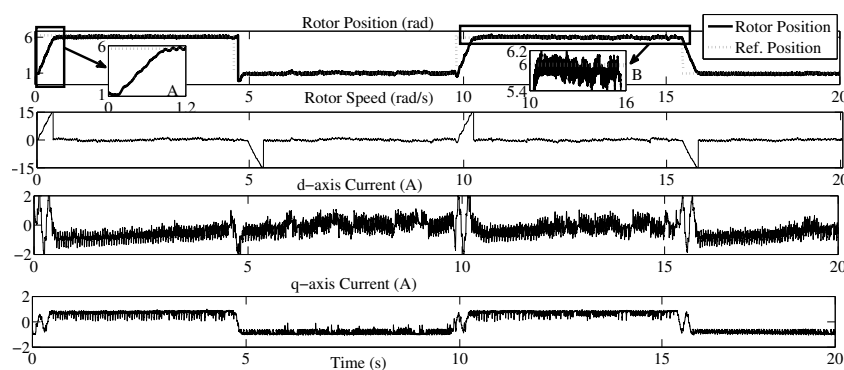

Figure 12. Experimental results for the system using the PID control strategy

The GPC strategy took about 2 seconds to settle, view detail A, with an oscillation of 0.4 radians, detail B. The rotor speed was characterized by medium values. The peak value of current i_{ds} did not exceed 2 A, while current i_{qs} has not assumed values greater than 1.5 A, as seen in Fig.13.
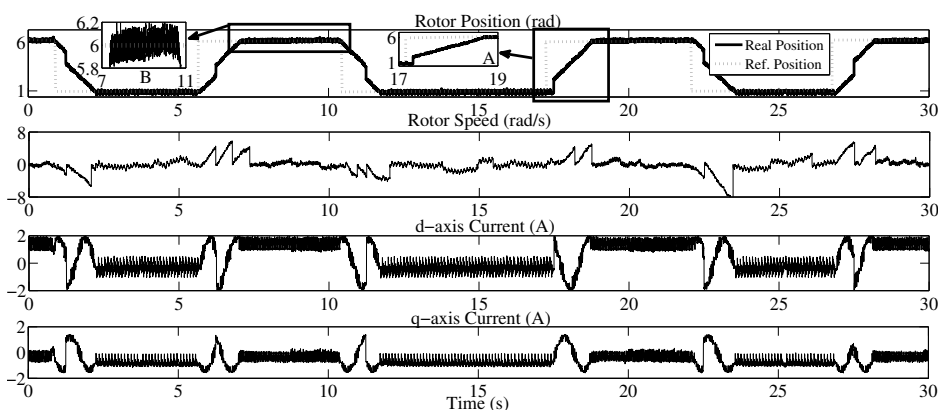

Figure 13. Experimental results for the system using the GPC control strategy

When the fuzzy technique is applied, 1.5 seconds are necessary to stabilize the reference around the desired value, detail A, which is similar to the PID case. Besides, the oscillation observed is similar to that in the GPC case, i.e. equal to 0.4 radians, detail B. The rotor speed displays a smooth behavior during the

settling time. It can be seen that current i_{ds} has a peak of 2 A, and current i_{qs} is also limited to 1 A in magnitude, according to Fig. 14.
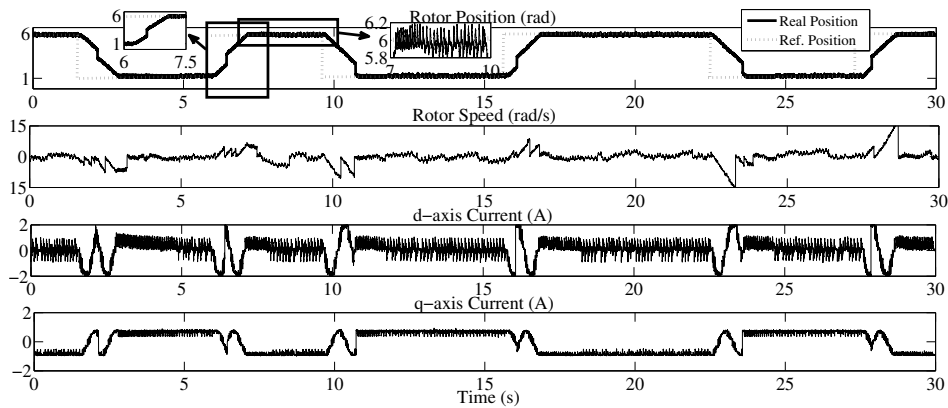

Figure 14. Experimental results for the system using the fuzzy control strategy

5.   Conclusion

Controlling the position of an induction machine is particularly difficult due to existing inertia moments and low viscous friction coefficient, which brings complexity to the control of rotor position. According to the obtained results, PID strategy showed the best performance among the studied techniques in the attempt of following the reference signal, but oscillations around the reference were observed. The GPC technique was then used in the studied system providing the expected results, with medium speed tracking to the reference and low swings in the steady state. By applying fuzzy technique, the rapid action in the following of the reference change, like in the PID strategy, was combined with low steady state oscillations achieved by GPC. Future work includes the search for a controller that reduces even further the oscillation of the rotor position in steady state condition. Some options to be investigated lie in the use of online GPC, GPC with disturbance rejection, or even a hybrid controller involving SMC and GPC. Finally, such techniques can be applied to a robotic arm, while actuation regarding other motor and controller types is expected to be also investigated.

References

Aguirre, L. A. (2004) *Introduo Identificao de Sistemas*. 1st edn, UFMG.

Åström, K., Hägglund, T. (1995) *PID Controllers: Theory, Design and Tunning*. Instrument Society of America.

Åström, K. and Hägglund T. (2006) *Advanced PID Control*. ISA–Instrumentation, Systems, and Automation Society.

BEERTEN, J., VERVECKKEN, J., DRIESEN. J. (2010) Predictive direct torque control for flux and torque ripple reduction. *IEEE Transactions on Industrial Electronics*, **57**, 404-412.

BOSE, B. K. (2001) *Modern Power Electronics and AC Drives.* 1st edn. Prentice Hall PTR.

CLARKE, D. W. (1987) Generalized predictive control: A robust self-tuning algorithm generalized predictive control. *Proc. of the 1987 American Control Conference*, American Automatic Control Council, Green Valley, AZ, 990-994.

COELHO, A. A. R., COELHO, L. S. (2004) *Identificao de sistemas dinamicos lineares*, 1st edn. Editora UFS.

DE SANTANA, E. S., BIM, E., DO AMARAL, W. C. (2008) A predictive algorithm for controlling speed and rotor flux of induction motor. *IEEE Transactions on Industrial Electronics* **55**, 4398-4407.

EGIGUREN, P. A., OSCAR, B. C. (2010) Robust position control of induction motor drives. *IEEE International Symposium on Industrial Electronics*, 1468-1473.

HALBAOUI, K., BOUKHETALA, D., BOUDJEMA, F. (2008) A new robust model reference adaptative control for induction motor drives using a hybrid controller. *Power Electronics, Electrical Drives, Automation and Motion 2008. SPEEDAM 2008. IEEE,* 1109-1113.

HO, T.-J., YEH, L.-Y. (2010) Design of a hybrid PID plus fuzzy controller for speed control of induction motors. *IEEE Conference on Industrial Electronics and Applications.* IEEE, 1352-1257.

HONÓRIO, D. A., DINIZ, E. C., DE SOUZA, A. B., ALMEIDA, O. M., BARRETO, L. H. S. C. (2010) Comparison between sliding mode and vector control for a DSP-Based position control applied to squirrel–cage induction motor. *IEEE/IAS International Conference on Industry Applications.* IEEE, 1-6.

JACOBINA, C. B., DE S. RIBEIRO, L. A., DE M. FILHO, J. B., SALVADORI, F., LIMA, A. M. N. (2003) Sistema de acionamento com motor de induo orientado indiretamente pelo campo com adaptao MRAC da velocidade. *Revista Controle & Automaço*, **14**, 41-49.

JÚNIOR, A. B. S. (2010) Estudo e implementao de um servoposicionador aplicando controle vetorial indireto a um motor de induo trifsico. Master's thesis. Univesidade Federal do Ceará, Fortaleza.

RAUTE, R., CARUANA, C., STAINES, C. S., CILIA, J., SUMNER, M., ASHER, G. M. (2010) Sensorless control of induction machines at low and zero speed by using PWM harmonics for Rotor–Bar slotting detection. *IEEE Transactions on Industry Applications*, **46**, 5, 1989-1998.

YING-YU T. (1996) DSP-Based robust control of an HAC induction servo drive for motion control. *IEEE Transactions on Control Systems Technology*, **4**, 614-625.

WAN, CH.-Y., KIM, S.-CH. AND BOSE, B.K. (1992) Robust position control of induction motor using fuzzy logic control. In: *Industry Applications*

Society Annual Meeting 1992. IEEE, 472–451.